JAAS

PAPER

View Article Online
View Journal | View Issue

Cite this: *J. Anal. At. Spectrom.*, 2025, **40**, 1754

Simultaneous determination of Cl, Br and I by aerosol-assisted PVG-ICP-MS†

Gustavo R. Bitencourt, [ab] Paola A. Mello, [a] Patricia Grinberg [*b] and Ralph E. Sturgeon [b]

Simultaneous determination of Cl, Br and I by aerosol-assisted photochemical vapor generation (PVG) with detection by inductively coupled plasma mass spectrometry (ICP-MS) was investigated. The photoreactor comprised a modified cyclonic spray chamber fitted with a central UV source for irradiation of pneumatically generated sample aerosol. A systematic evaluation of variables was conducted, focusing on achieving compromise optimal PVG conditions suitable for simultaneous Cl, Br and I generation. By using a sample medium comprising 1% v/v acetic acid containing 20 mg L^{-1} Cu^{2+} as mediator, the signal intensities for Cl, Br and I were enhanced by 3-, 40- and 30-fold, respectively, compared to those obtained by conventional pneumatic nebulization (PN). LODs of 4.2 ng mL^{-1}, 6.3 pg mL^{-1} and 1.9 pg mL^{-1} were achieved for Cl, Br and I, respectively, with corresponding estimated overall PVG efficiencies of 10, 99 and 90%. In addition to the halides, halate species, *i.e.*, ClO_3^-, BrO_3^- and IO_3^-, were also examined, but poor PVG efficiencies (lower than 5%) were encountered. However, addition of 20 mg L^{-1} SO_3^{2-} to the generation medium enhanced response for BrO_3^- and IO_3^-, achieving similar values to those obtained from Br^- and I^-. The impact of NO_3^- (as both HNO_3 and KNO_3) and NH_4OH on generation efficiencies was also investigated. The method was tested by the successful simultaneous determination of total Cl, Br and I in a variety of certified reference materials (CRMs) digested by microwave-induced combustion (MIC), including NRCC DORM-5 – Fish Protein, NIST SRM 1632c – Coal, NIST SRM 1515 – Apple Leaves and NIST SRM 1549 – Non-fat Milk Powder.

Received 27th February 2025
Accepted 13th May 2025

DOI: 10.1039/d5ja00079c

rsc.li/jaas

1 Introduction

Chlorine, bromine and iodine are present in a wide variety of food, biological, clinical, industrial and environmental samples. Their concentration range and chemical species define the benefits or toxicity for humans, their impact on the environment, as well as use in industry.[1] Chlorine is considered an essential element for humans (as Cl^-) and has an important role in living cells and is often present at high concentrations in most samples. High concentrations of Cl^- in water can cause corrosion or clogging of metallic pipes and even at trace levels may damage device fabrication in the electronics and semiconductor industries.[2,3] Bromine is present at trace levels in the human body, but its role remains uncertain. While some benefits have been demonstrated, such as in the development of tissue and collagen structure,[4] or as an antiepileptic agent,[5] bromine can competitively reduce iodine accumulation in the thyroid and skin when present at high levels, in addition to increasing iodine excretion by the kidneys.[6] Iodine is a micronutrient essential for human metabolism, crucial to synthesis of thyroid hormones. Its deficiency or excess exposure can induce a range of disorders, including hypo- or hyperthyroidism, as well as other clinical abnormalities.[7]

It is clear that routine determination of Cl, Br and I in a variety of matrices is essential, requiring analytical techniques capable of addressing trace level concentrations. Several techniques have been used, including ion chromatography (IC) with conductivity detection,[8–10] gas chromatography mass spectrometry (GC-MS),[11–13] X-ray fluorescence spectrometry (XRF),[14,15] high-resolution continuum source atomic absorption spectrometry (HR-CS-AAS),[16–18] inductively coupled plasma optical emission spectrometry (ICP-OES)[19,20] and inductively coupled plasma mass spectrometry (ICP-MS),[21,22] among others.[23] Of these techniques, ICP-MS is particularly noteworthy due to its superior limits of detection (LODs).[1] However, several shortcomings impair halogen detection by ICP-MS, including their high ionization potentials (12.9, 11.8 and 10.5 eV for Cl, Br and I, respectively) with consequent low degree of ionization, severe memory effects, and potential spectral interferences from both sample matrix concomitants and typical plasma ions (*e.g.*, $^{18}O^{16}O^1H^+$, $^{38}Ar^{40}Ar^1H^+$ and $^{40}Ar^{40}Ar^1H^+$ generating isobaric interferences on ^{35}Cl, ^{79}Br and ^{81}Br, respectively).

[a]*Departamento de Química, Universidade Federal de Santa Maria, Santa Maria, RS, 97105-900, Brazil*

[b]*Metrology Research Centre, National Research Council Canada, Ottawa, ON, K1A 0R6, Canada. E-mail: Patricia.Grinberg@nrc-cnrc.gc.ca*

† Electronic supplementary information (ESI) available. See DOI: https://doi.org/10.1039/d5ja00079c

Furthermore, the poor sample nebulization efficiency (typically 2–3%) provided by conventional pneumatic nebulization (PN) further limits potential LODs.[1,24]

To overcome some such shortcomings, use of photochemical vapor generation (PVG) for analyte introduction has been the focus of significant research over the past two decades. Production of volatile analyte species induced by UV photolysis of aqueous solutions typically containing added low-molecular-weight organic acids (*e.g.*, acetic acid), has been successfully utilized for the determination of numerous metals and non-metals, including the halogens.[25–27]

Iodine is recognized as the halogen most readily amenable to PVG.[28,29] In the presence of 5% v/v acetic acid and under UV-C irradiation, an estimated generation efficiency of 94% is achieved,[29] yielding a 40-fold enhancement of the LOD compared to that obtained by PN. PVG methodology was validated through analysis of several different sample matrices.[28] In another study, the ethanol content in alcoholic beverages was used to produce radicals through UV irradiation, thereby enabling direct photochemical generation of iodine, enhancing sensitivity 64% over that arising from PN.[30] Photochemical generation of Br was successfully achieved from a 2% v/v acetic acid solution containing 3 mg L^{-1} NH_4Cl. The NH_4^+ ions were hypothesized to serve as electron scavengers, enhancing PVG efficiency to yield a 17-fold improvement in the LOD compared to that with PN, and a generation efficiency of 95%. Determination of Br in IRMM BCR-611 (Low Level Bromide in Groundwater), NIST SRM 1568b (Rice Flour), and SRM 1632 (Bituminous Coal) reference materials was successfully demonstrated.[31]

PVG of Cl^- is not possible based on the conditions utilized for I^- and Br^-. Under UV-C irradiation, photochemical transformation of X^- (X = Br or I) occurs *via* a charge transfer-to-solvent process (CTTS), resulting in the formation of a cage complex comprising $X^\bullet$ and solvated electrons ($e^-_{(aq)}$). Subsequently, $X^\bullet$ interacts with $H_3C^\bullet$ arising from the photolysis of acetic acid present in solution, generating volatile CH_3X.[26] Emission from the UV source, limited to 185 nm, cannot excite a CTTS process for chloride due to its short UV absorption line (177.6 nm). However, a metal-ion assisted/mediated PVG reaction can be successfully conducted.[26] Prior studies have demonstrated their impact in enhancing PVG efficiencies of the halogens, including the use of added Cu^{2+} for F, Cl and Br,[2,32,33] Co^{2+} for Br[32] and Fe^{3+} for Cl and Br.[34,35] The added metal ions alter the mechanism of the reaction by formation of a Cu–X complex (X = Cl or Br), which can be excited by UV-B (longer wavelength) to undergo an efficient ligand-to-metal charge transfer process, yielding $X^\bullet$ to permit subsequent formation of CH_3X.[32,36] Using 1% v/v acetic acid and 7.5 μg g^{-1} Cu^{2+}, a 74-fold enhancement in sensitivity for Cl^- was obtained compared to PN.[2] For Br^-, generation efficiencies of 92% and 94% were achieved using a flow-through lamp (emitting at 185 and 254 nm) and a simple germicidal lamp (emitting at 254 nm), respectively, from a 2% v/v acetic acid medium in the presence of 10 mg L^{-1} Cu^{2+}.[32] Generation of volatile Cl^- and Br^- (in addition to F^-) species was also reported from a simple copper acetate solution, resulting in their effective PVG from a so-called "organic acid-free" medium.[37]

Typically, PVG hardware comprises a photoreactor and a tandem gas–liquid phase separator (GLS) to ensure efficient release of generated volatile species from the irradiated liquid medium, which are then directed to the detection system by a carrier gas.[26] This setup has been used in most of the aforementioned studies of halogen generation, wherein the photoreactor is a high efficiency flow-through low pressure mercury discharge lamp emitting both 254 and 185 nm Hg lines. Nevertheless, other photoreactors have been shown to be well-suited for PVG systems, including simpler germicidal lamps. Of particular interest for this study is a relatively unexplored combined UV-assisted spray chamber[38] introduced nearly two decades ago, consisting of a standard cyclonic spray chamber modified to accommodate a central UV-C pen lamp. In addition to the absence of any perturbation to operation of the spray chamber using conventional PN sample introduction, this photoreactor offers the advantage of a direct ICP-MS compatible assembly that simplifies PVG operation.

The sparse number of studies using the UV-assisted spray chamber[28,29,38,39] is likely linked to a number of significant shortcomings inherent to the system, such as the elimination of the gas–liquid phase separation feature which serves to minimize introduction of sample matrix (a notable advantage of vapor generation techniques), the relatively brief analyte residence time within the spray chamber, yielding UV irradiation times on the order of only 3 s, and the need to generate a fine aerosol, which limits solution uptake rates and eliminates the advantages of high vapor flux processing (*i.e.*, solution flow rates limited to <1 mL min^{-1}). While potential detrimental matrix effects impacting the photochemical reactions and analyte detection by ICP-MS can be mitigated by various means, such as simple sample dilution, use of reaction/collision cells, reliance on internal standards and application of isotope dilution, or the employment of an appropriate sample preparation method,[1] the limited irradiation time represents an inherent constraint that must be overcome through reliance on optimized PVG conditions. Noteworthy in this context is that the interaction between analytes, reducing species and UV radiation within aerosolized microdroplets generated by PN could potentially accelerate the kinetics of photochemical (and other) reactions,[40–42] thereby offsetting the detrimental impact of short irradiation times.

The purpose of the present study was to develop a suitable method for the simultaneous determination of chlorine, bromine and iodine by aerosol-assisted PVG-ICP-MS using the convenience of a UV-assisted spray chamber. A systematic evaluation of PVG conditions was undertaken, focused on identifying suitable compromise conditions. The resultant fit-for-purpose methodology was demonstrated through the analyses of a variety of certified matrix reference materials (CRMs) digested by microwave-induced combustion (MIC).

2 Experimental

2.1 Instrumentation

A schematic diagram of the PVG system used in this work is illustrated in Fig. 1. The photoreactor consisted of a 50 mL

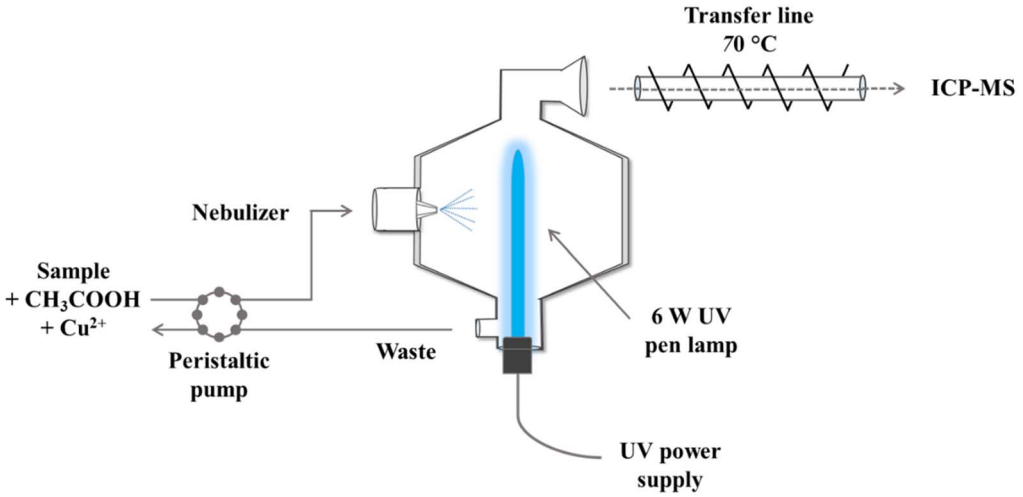

Fig. 1 Schematic of the PVG-ICP-MS system.

internal volume water-jacketed cyclonic spray chamber (Glass Expansion, Australia) in which the standard waste removal line was adapted to accommodate a 6 W Analamp mercury UV-C source emitting at 254 and 185 nm (model 81-1057-51, BHK Inc., Canada).[38] Sample solution was delivered at 1 mL min^{-1} through a glass concentric nebulizer (Meinhard, USA) *via* a peristaltic pump. As the vertical dimension of the photoreactor was larger than the stand-alone spray chamber, its direct coupling to the base of the injector torch necessitated use of a short ball-and-socket glass transfer line (length of 20 cm and i.d. of 5 mm). This line was maintained at 70 °C through the use of a heating tape in order to prevent moisture condensation. All measurements were undertaken using an Elan® DRC II inductively coupled plasma mass spectrometer (PerkinElmer-Sciex, Canada) fitted with conventional Ni sampler/skimmer cones. The ICP-MS operating conditions are summarized in Table 1.

A Multiwave 5000 microwave sample preparation system (Anton Paar, Austria) was used for sample digestion by MIC. The microwave system was operated at its maximum power, temperature and pressure of 1500 W, 280 °C and 80 bar, respectively. The system is equipped with eight high-pressure quartz vessels each of 80 mL internal volume. Commercial quartz sample holders (Anton Paar) were used to accommodate sample pellets for combustion.

Table 1 Operating parameters for the determination of Cl, Br and I by PVG-ICP-MS

Parameter	ICP-MS
RF power, W	1300
Nebulizer gas flow rate, L min^{-1}	1.15
Auxiliary gas flow rate, L min^{-1}	1.1
Plasma gas flow rate, L min^{-1}	17.5
Sample flow rate, mL min^{-1}	1.0
Measurement mode	Peak hopping
Dwell time, ms	50
Replicates	5
Isotopes monitored, *m*/*z*	^{35}Cl, ^{79}Br, ^{81}Br, ^{127}I

All statistical evaluations and data manipulation were performed using GraphPad InStat software (GraphPad InStat Inc, Version 3.06, 2007); confidence levels of 95% were accepted.

2.2 Reagents, standards and certified reference materials

Ultrapure water obtained from a Milli-Q Advantage system (18.2 MΩ cm, Millipore Sigma, USA) was used for preparation of all working solutions. Both ACS-grade (≥99.7%, Fisher Scientific, Canada) and TAMA Pure AA-100 (TAMA Chemical Inc., Japan) acetic acid were used. Ammonium hydroxide, ACS grade (28 to 30%), was obtained from Fisher Scientific (Canada). For MIC procedures, a 3.0 mol L^{-1} solution of NH_4NO_3 was prepared from its respective salt (Merck, Germany) and used as the combustion igniter. Oxygen (99.5%, White Martins, Brazil) was used to pressurize the digestion vessels to 20 bar. Small discs of filter paper (15 mm diameter, about 12 mg) with low ash content (Black Ribbon Ashless, Schleicher and Schuell, Germany) were used to aid the combustion process. The filter paper was previously cleaned with ethanol (Merck, Brazil) for 20 min in an ultrasonic bath, rinsed with water and dried in a class 100 laminar bench (CSLH-12, Veco, Brazil) before use. Nitric acid (Fisher Scientific, Canada), in-house double-distilled by a sub-boiling system, and potassium nitrate (Anachemia Chemicals, Canada) were used to evaluate potential interferences from NO_3^-. Sodium sulfite (Caledon Laboratories Ltd., Canada) was evaluated for reduction of ClO_3^-, BrO_3^- and IO_3^- species.

Stock solutions of 1000 mg L^{-1} of Cl^-, Br^- and I^- were prepared by dissolving their sodium salts (Anachemia Chemicals, all analytical-grade) in ultrapure water. Additionally, stock solutions (1000 mg L^{-1}) of ClO_3^-, BrO_3^- and IO_3^- were prepared by dissolving potassium chlorate, sodium bromate and sodium iodate (Anachemia Chemicals, all analytical-grade), respectively, in ultrapure water. These reagents were dried at 105 °C in an air convection oven for 2 h and cooled in a desiccator prior to gravimetric preparation of individual nominal 1000 mg L^{-1} stock solutions. Working solutions were prepared daily by diluting the stock solutions with appropriate concentrations of acetic acid.

A stock solution of nominal 5000 mg L^{-1} of Cu^{2+} was prepared by dissolving a high-purity copper wire certified reference material (NRC CRM HICU-1, 99.999%, National Research Council, Canada) in 30% v/v double-distilled nitric acid. In order to minimize the final NO_3^- concentration, the copper solution was carefully evaporated in a class 100 clean hood and the salt reconstituted with 1% v/v acetic acid.

Four certified reference materials (CRMs) were selected to evaluate the performance of the proposed procedure: NRCC CRM DORM-5 Fish Protein (National Research Council Canada, Canada), NIST SRM 1632c Coal, NIST SRM 1515 Apple leaves and NIST SRM 1549 Non-fat milk powder (National Institute of Standards and Technology, USA). In accordance with their certificates, dry weight corrections for moisture content were determined by drying separate subsamples of each material at 60 °C in a conventional oven (Nova Ética, Brazil) until constant weight was achieved. For MIC digestion, samples were pressed for 3 min into pellets (diameter of 13 mm) using a hydraulic press (Specac, UK) set at 5 ton.

2.3 Analytical procedures

2.3.1 Optimization of PVG-ICP-MS parameters. A multielement solution was used for tuning the ICP-MS, as recommended by the manufacturer. Subsequently, optimized RF plasma power and nebulizer gas flow rate parameters were determined using PN and set to 1300 W and 1.15 L min^{-1}, respectively, for detection of ^{35}Cl, ^{79}Br, ^{81}Br and ^{127}I. For all evaluations throughout this study, a sample flow rate of 1 mL min^{-1} was maintained.

Unless otherwise specified, optimization of the PVG parameters was conducted using multielement test solutions containing 5 mg L^{-1} Cl^-, 10 μg L^{-1} Br^- and 2 μg L^{-1} I^- to ensure adequate precision of measurement. These same concentrations were used when experiments with ClO_3^-, BrO_3^- and IO_3^- species were undertaken. As the purpose of this work was to develop a method for simultaneous determination of Cl, Br and I using PVG sample introduction, all parameters were evaluated using both individual and mixed solutions of the analytes to ascertain whether cross-element interactions influenced their generation. For the PVG parameters, the effect of the acetic acid concentration in the range 0.25 to 10% v/v and of the amount of added Cu^{2+} mediator (in range from 5 to 100 mg L^{-1}) were evaluated. Potential interferences induced by NO_3^- present in the range 1 to 100 mmol L^{-1} (as HNO_3 or KNO_3) and by NH_4OH (0.1 to 200 mmol L^{-1}) on PVG efficiencies were also investigated. Use of SO_3^{2-} for the reduction of ClO_3^-, BrO_3^- and IO_3^- was examined in the range 5 to 100 mg L^{-1} in 1% v/v acetic acid containing 20 mg L^{-1} Cu^{2+}.

2.3.2 Sample preparation. MIC was used for sample preparation of solid samples following procedures based on previous reports.[43,44] Nominal 200 mg sample pellets were weighed and transferred to quartz holders containing filter paper discs moistened with 50 μL of 3 mol L^{-1} NH_4NO_3 igniter solution. The quartz holders were then inserted into quartz digestion vessels previously charged with 6 mL of 50 mmol L^{-1} NH_4OH which served as the absorber medium. After closing the vessels and placing them in the rotor, they were pressurized to 20 bar with oxygen and submitted to microwave irradiation at 900 W for 5 min. The digests were quantitatively transferred to volumetric flasks after being cooled to room temperature, and diluted to 25 mL with ultrapure water.

2.4 Safety considerations

The full range and identity of volatile compounds produced during PVG is unknown. Standard safety precautions should be taken during all experiments and an adequate ventilation/exhaust system should be used.

3 Results and discussion

3.1 Optimization of PVG conditions using acetic acid and Cu^{2+} as ion mediator

Preliminary investigations were devoted to evaluation of the signals arising from PN of an aqueous multi-standard solution generated in the physical presence and absence of the UV pen lamp. No statistical differences between signal intensities were detected (*t* test, 95% confidence level). Furthermore, all experiments performed during method optimization were also undertaken using both single and mixed solutions of the halogens with any differences being less than 10% (data not shown). Thus, results obtained based on a multi-standard solution were used for all subsequent studies.

An acetic acid medium is commonly used for PVG of the halogens as the production of water-soluble acids (HX) and poorly volatile species (C_2H_5X) impairs the use of formic and propionic acids, respectively.[2,26,31] Acetic acid was thus solely evaluated as the generation medium in this study.

Fig. 2 illustrates the time evolution of signal profiles obtained from solutions containing 5 mg L^{-1} Cl^-, 10 μg L^{-1} Br^- and 2 μg L^{-1} I^- in 1% v/v acetic acid (dotted lines without Cu^{2+} and solid lines with 20 mg L^{-1} Cu^{2+}). Conventional PN intensities are recorded for 50–60 s before the UV lamp is powered on and serve to illustrate the reference signals arising in the absence of photochemical processes. As evident in Fig. 2A, there is no difference in the steady-state Cl^- signal intensity obtained in only acetic acid whether the aerosol is subjected to UV irradiation or not (compare dotted line intensities before and after the lamp is powered on). As noted earlier, the short UV absorption line of Cl^- (177.6 nm band maximum) precludes its overlap with any emission lines from the UV source and hence no photochemical reaction develops. For Br^- and I^-, enhancement factors of 5- and 30-fold are evident in Fig. 2B and C, respectively, when the UV lamp is powered on. Although the UV pen lamp emits at 185 nm, the poor overlap with the absorption band maximum for Br^- (*i.e.*, 197.8 nm), and the relatively short irradiation time (approximately 3 s) in the spray chamber, limits the extent of photochemical reactions leading to CH_3Br generation. Iodine is the most readily responsive halogen for PVG as its absorption band maximum is at 226 nm. Its 30-fold signal enhancement factor is in agreement with that reported in previous studies.[28,29]

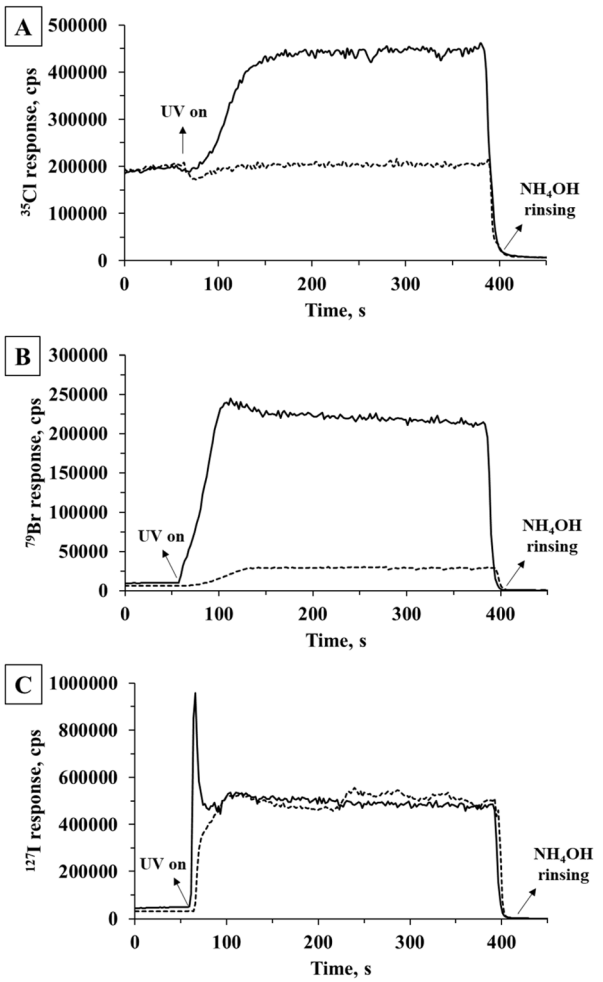

Fig. 2 PVG-ICP-MS response from a multi-element solution of (A) 5 mg L^{-1} Cl^-, (B) 10 μg L^{-1} Br^- and (C) 2 μg L^{-1} I^- in 1% v/v acetic acid (dotted line) and 1% acetic acid containing 20 mg L^{-1} Cu^{2+} (solid line). A 5% v/v NH_4OH solution was used to rinse the system to minimize carryover.

The presence of Cu^{2+} has earlier been shown to enhance the PVG efficiency for Cl^- and Br^-.[2,32] It is clear from Fig. 2A and B that when the UV lamp is powered on, PVG responses for Cl^- and Br^- are enhanced 3- and 40-fold, respectively. No additional PVG enhancement is evident for I^- in the presence of Cu^{2+} (Fig. 2C) because CH_3I is already efficiently generated from the 1% v/v acetic acid medium. The impact of added Cu^{2+} on PVG response from Cl^- is significantly lower than that earlier reported by Hu *et al.*[2] (74-fold; 43-fold normalized to 1.0 mL min^{-1}), highlighting the consequence of the brief aerosol UV irradiation time within the spray chamber (≈3 s) compared to that in a flow-through lamp (45 seconds at a sample flow rate of 1.7 mL min^{-1}).

Noteworthy is that in all cases, PVG signal intensities increase the moment the solution is irradiated, but it is evident that this occurs at different rates for each halogen. A pronounced spike occurs for I^- and was attributed to the intense irradiation of species adsorbed on the cool UV pen lamp surface prior to powering it.[29] This spiking was not evident if the UV lamp was permitted to stabilize for 20 min before analytical measurements were recorded, supporting this supposition. For reasons unknown, the spike was only observed when Cu^{2+} was present in the solution. Signals for Br^- and Cl^- increased more slowly, possibly a result of the warming of the UV lamp leading to temporally increasing intensities of the shorter 185 nm UV radiation required to effect PVG of these elements.[45]

Optimization studies were conducted to evaluate the effect of varying concentrations of acetic acid and Cu^{2+} on PVG response; results are shown in Fig. 3 and 4 for processing multielement solutions. Optimal response for Br^- was obtained using 0.25% v/v acetic acid, whereas 1% v/v was evident for Cl^- and I^-. Higher concentrations led to a notable decrease in all signals, possibly due to spectral shadowing in the presence of this absorber, leading to a decreasing depth of penetration of short UV photons into the liquid medium at higher concentrations of acetic acid.[25] A concentration of 1% v/v acetic acid was selected as a compromise for further evaluation.

Fig. 4 shows that addition of increasing concentrations of Cu^{2+} enhances the response for Cl^-, demonstrating its crucial role as a mediator for CH_3Cl generation.[2] Highest signal intensity for Br^- was obtained in the presence of 10 mg L^{-1} Cu^{2+}, and no significant decline in response occurred even at concentrations exceeding 20 mg L^{-1} (maximum signal suppression at 100 mg L^{-1} Cu^{2+} was about 10%). The intensity of the signal for I^- obtained with 5 and 10 mg L^{-1} Cu^{2+} was only 15% higher than that generated in its absence, indicating that Cu^{2+} may also serve to slightly enhance PVG efficiency of I^- when using an aerosol-assisted process, kinetically compensating for the reduced UV exposure time. At 20 mg L^{-1} Cu^{2+}, response from I^- was identical to that observed using only 1% v/v acetic acid. On the other hand, a remarkable decrease was noted with higher Cu^{2+} concentrations, suggesting that it may interfere with the generation of CH_3I due to a possible further spectral shadowing effect (*i.e.*, decrease in photon penetration depth). As such, 20 mg L^{-1} Cu^{2+} was selected as the optimal compromise concentration for further evaluations, based on a sacrifice in response from I^- due to its intrinsically higher generation efficiency.

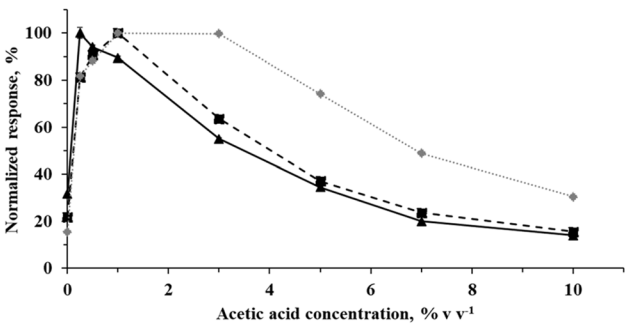

Fig. 3 Effect of acetic acid concentration (in the presence of 20 mg L^{-1} Cu^{2+}) on the normalized response from a multi-element solution containing Cl^- (5 mg L^{-1}, -■-), Br^- (10 μg L^{-1}, —▲—) and I^- (2 μg L^{-1}, ···◆···). Error bars presenting the standard deviation (n = 3) are typically buried within the signal marker.

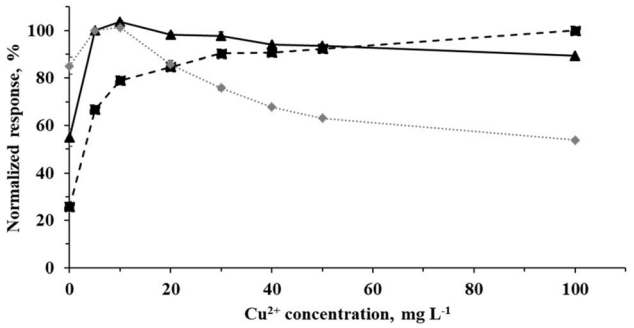

Fig. 4 Effect of Cu^{2+} concentration (in the presence of 1% v/v acetic acid) on the normalized response from a multi-element solution containing Cl^- (5 mg L^{-1}, ▬■▬), Br^- (10 μg L^{-1}, ▬▲▬) and I^- (2 μg L^{-1}, ···◆···). Error bars presenting the standard deviation ($n = 3$) are typically buried within the signal marker.

No memory effects were evident following rinsing of the system with 5% v/v NH_4OH for 2 min between samples. However, it is noteworthy that use of the rinse solution resulted in a slower recovery of the Cl signal intensity compared to its more rapid stabilization achieved when the system had not been previously exposed to NaOH, as shown in Fig. 5. This may be attributed to the time required for the interior surface of the spray chamber to become equilibrated with the sample (*cf.* Section 3.3, consistent with interferences from NH_4OH on PVG of Cl^-). Data acquisition was thus started following a minimum 2 min of sample introduction or until a signal precision better than 2% for all analytes was attained.

3.2 Interferences during simultaneous PVG of halogens

Development of a method for simultaneous PVG of multiple elements is a challenge, especially considering halogens and their species specific generation efficiencies.[2] Although HNO_3 is less commonly used for solubilization and stabilization of halogens, its effects can be problematic and must be investigated. The photolysis of NO_3^- generates multiple oxidizing species that consume reductive radicals ($e_{(aq)}^-$, $H^\bullet$ and $R^\bullet$) that are often required for the PVG process.[46] In this context, the influence of both NO_3^- (a possible concomitant present in sample digests) and NH_4OH (a common solution selected for halogen extraction in several matrices) were evaluated.

Firstly, the influence of NO_3^- on the photochemical generation of Cl^-, Br^- and I^- was undertaken using HNO_3 present at concentrations ranging from 1 to 500 mmol L^{-1} in a medium of 1% acetic acid and 20 mg L^{-1} Cu^{2+}. As illustrated in Fig. 6A, Cl^- demonstrated good tolerance up to 500 mmol L^{-1} HNO_3, with only 7% signal suppression. PVG of Br^- was affected at HNO_3 concentrations exceeding 100 mmol L^{-1}, with a notable 53% suppression at 500 mmol L^{-1}. On the other hand, the addition of only 5 mmol L^{-1} HNO_3 led to a 14% reduction of the I^- signal. These findings differ from those of previous studies[2,32] in

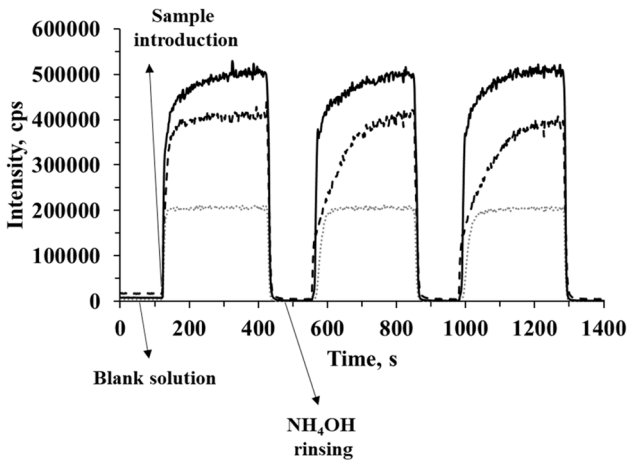

Fig. 5 Effect of the 5% v/v NH_4OH rinse solution on the signals from 2 μg L^{-1} I^- (solid black line), 5 mg L^{-1} Cl^- (dashed black line) and 10 μg L^{-1} Br^- (dotted gray line) in 1% v/v acetic acid + 20 mg L^{-1} Cu^{2+}. Note that 5% v/v NH_4OH was introduced as a rinse between the successive replicate sample introductions.

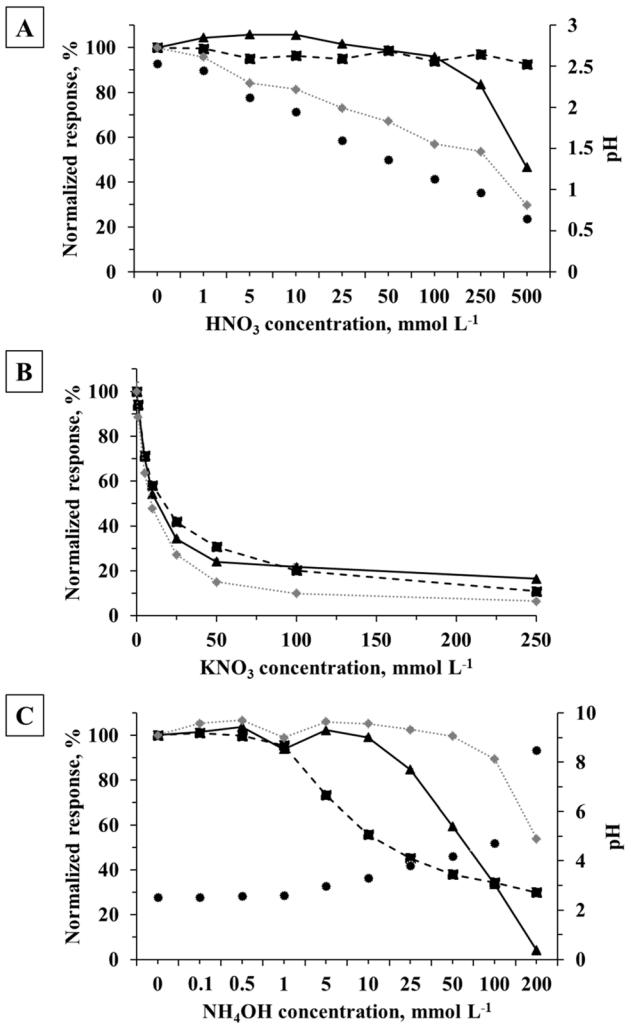

Fig. 6 Effects of NO_3^- added as HNO_3 (A) or KNO_3 (B), and NH_4OH (C) on PVG of 5 mg L^{-1} Cl^- (▬■▬), 10 μg L^{-1} Br^- (···◆···) and 2 μg L^{-1} I^- (···◆···). Secondary ordinate represents solution pH (●). Error bars presenting the standard deviation ($n = 3$) are typically buried within the signal marker.

which Cl^- and Br^- generation efficiencies were reduced even in the presence of 15 mmol L^{-1} HNO_3 (Cu^{2+} was used as mediator in both cases) using a flow-through lamp as the photochemical reactor. The brief residence time within the UV-assisted spray chamber must be considered a possible factor in mitigating the effects of HNO_3 on their generation efficiencies. When selecting the sources of NO_3^- it is important to consider that the preparation of the Cu^{2+} solution from high purity copper involved its dissolution in 5% v/v HNO_3, yielding a 3 mmol L^{-1} HNO_3 concentration in the working solutions (20 mg L^{-1} Cu^{2+}). At this concentration, a negligible effect of HNO_3 on the generation of Cl^- and Br^- is expected. However, the higher susceptibility of I^- to the presence of HNO_3 required evaporation of the Cu^{2+} solution to near dryness and its subsequent reconstitution in 1% v/v acetic acid to readily avoid this source of interference.

The presence of higher concentrations of HNO_3 also decreases the pH of the test solutions (● in Fig. 6A). To assess the isolated impact of NO_3^- ions, further information was obtained by examining interference from NO_3^- derived from KNO_3 (Fig. 6B). The effect of NO_3^- was significantly more pronounced in the form of added KNO_3 compared to that for HNO_3. Even at a concentration of 1 mmol L^{-1} KNO_3, severe interference was evident (*i.e.*, 11% suppression for I^-). Comparing the effects of the two sources of NO_3^- (HNO_3 and KNO_3) suggests that the pH of the solution plays a significant role in PVG of the halides. As expected, addition of KNO_3 to the reaction media had no impact on solution pH. Minimizing excess H^+ through use of KNO_3 instead of HNO_3 may reduce formation of $H^\bullet$ which may lead to "unproductive" generation of XH species, reducing analyte response.

The performance of the developed PVG methodology was examined by the analysis of various matrix CRMs subjected to prior MIC digestion (Section 3.6), utilized in an effort to minimize residual nitrate. As NH_4OH is used as the absorbing solution, its impact on subsequent halide generation was investigated (Fig. 6C). Solutions of 1% v/v acetic acid and 20 mg L^{-1} Cu^{2+} containing NH_4OH ranging from 0.1 to 200 mmol L^{-1} were examined. As with HNO_3, the pH of the solutions is strongly influenced by the NH_4OH concentration. At 200 mmol L^{-1}, the pH was higher than 8, and the solution exhibited a light blue color. At alkaline pH, Cu^{2+} forms a $Cu(OH)_2$ precipitate, even at low concentrations of NH_4OH. Excess NH_4OH forms a dark blue $[Cu(NH_3)_4]^{2+}$ complex.[47] A substantial decrease in Cl^- PVG signal (the halide most dependent on the added Cu^{2+}) occurs in the presence of 5 mmol L^{-1} NH_4OH (pH 3). Also dependent on Cu^{2+}, PVG response for Br^- is suppressed in solutions containing more than 25 mmol L^{-1} NH_4OH. In the case of PVG of I^-, which efficiently occurs even in the absence of Cu^{2+}, suppression was evident only in the range of 200 mmol L^{-1} NH_4OH and likely due to uncharacterized effects on the photochemical reactions that occur under alkaline conditions.

3.3 PVG of ClO_3^-, BrO_3^- and IO_3^- species

Photochemical reactions involving chlorate (ClO_3^-), bromate (BrO_3^-) and iodate (IO_3^-) anions present some kinetic limitations, resulting in different generation rates when compared with their corresponding halides.[36] The impact of these species on their PVG using the UV-assisted spray chamber was investigated using earlier optimized conditions (*i.e.*, 1% v/v acetic acid + 20 mg L^{-1} Cu^{2+}). Poor generation efficiencies for all the investigated halate species arise, with only 3- and 2-fold enhancements obtained for BrO_3^- and IO_3^- compared to their conventional solution PN, whereas chlorate provides no PVG response. Although prior studies have reported higher generation efficiencies for ClO_3^-,[2] BrO_3^- (ref. 31 and 32) and IO_3^-,[28,29] the majority have employed a flow-through lamp providing a significantly longer irradiation time than that possible in the UV-assisted spray chamber, highlighting the slow kinetics of their stepwise photochemical reactions. Additionally, the previous studies comprising PVG of I from IO_3^- did not employ any metal mediator, which functions as an interference in this case. This is evidenced in Fig. S3 (ESI†), wherein no difference was observed for the signals obtained for I^- and IO_3^- in the 1% v/v acetic acid medium whereas a significant decrease occurs for IO_3^- in the presence of 20 mg L^{-1} Cu^{2+}.

The potential use of UV/SO_3^{2-}-based advanced reduction processes (ARPs) has been widely explored for the degradation of a range of environmental contaminants, including BrO_3^-.[48,49] Under UV irradiation, SO_3^{2-} and HSO_3^- give rise to the formation of $e_{(aq)}^-$, $H^\bullet$ and $SO_3^{-\bullet}$ radicals. In addition to the generation of successively reduced Br species from BrO_3^- (bromite, hypobromite and bromide) mediated by $e_{(aq)}^-$ and $H^\bullet$, H_2SO_3 and HSO_3^- may also be involved in BrO_3^- reduction, as illustrated by eqn (1)–(5).[48]

$$BrO_3^- + H_2SO_3 \rightarrow SO_3^{-\bullet} + BrO_2 + H_2O \quad (1)$$

$$2BrO_2 + HSO_3^- + H_2O \rightarrow 2HBrO_2 + SO_4^{2-} + H^+ \quad (2)$$

$$2BrO_2 + H_2O \rightarrow HBrO_2 + BrO_3^- + H^+ \quad (3)$$

$$HBrO_2 + HSO_3^- \rightarrow HOBr + SO_4^{2-} + H^+ \quad (4)$$

$$HOBr + HSO_3^- \rightarrow Br^- + SO_4^{2-} + 2H^+ \quad (5)$$

Noteworthy is that Br^- and SO_4^{2-} are the final products that remain following the treatment of BrO_3^- by UV/SO_3^{2-}. Although not yet studied, it is reasonable to hypothesize that such reactions may also apply to ClO_3^- and IO_3^- species. Thus, the potential of SO_3^{2-} as an adjuvant for the generation of methyl halides from their halate forms (either with the addition of Cu^{2+} or not) was investigated. The impact of UV/SO_3^{2-} treatment on PVG of Cl^-, Br^- and I^- species was concomitantly evaluated to ensure that no new interferences were encountered.

As can be seen in Fig. S1–S3 (ESI†), the presence of 100 mg L^{-1} SO_3^{2-} in a 1% v/v acetic acid medium did not affect signals from Cl^- and Br^-, but a detrimental effect on PVG of I^- and IO_3^- was clear. Significant suppression of PVG response for all the halides was encountered when SO_3^{2-} was present in solutions also containing 20 mg L^{-1} Cu^{2+}. On the other hand, an enhancement in generation efficiency from BrO_3^- and IO_3^- was achieved in the presence of added SO_3^{2-}, resulting in signal intensities comparable to those observed for Br^- and I^-.

Unfortunately, response from ClO_3^- remains essentially unaltered despite the presence of added SO_3^{2-}.

The influence of the concentration of SO_3^{2-} added to the acetic acid/Cu^{2+} generation medium was evaluated over a range from 1 to 100 mg L^{-1} with the objective of seeking an optimal condition exhibiting minimal suppression effects on the halides in conjunction with the greatest enhancement in PVG response for the halates. Results are presented in Fig. 7.

In the case of ClO_3^-, a maximum 16% signal increase was achieved in the presence of 20 mg L^{-1} SO_3^{2-} (Fig. 7A). Although degradation of ClO_4^- *via* a ClO_3^- intermediate to ultimately yield Cl^- is feasible with bulk radiolysis,[48] use of SO_3^{2-} is apparently not efficient for the rapid reduction of ClO_3^- when using the UV-assisted spray chamber. It was also evident that the baseline for ^{35}Cl in the presence of 100 mg L^{-1} SO_3^{2-} increased about 3-fold, likely due to the generation of a $^{34}S^1H^+$ polyatomic ion.

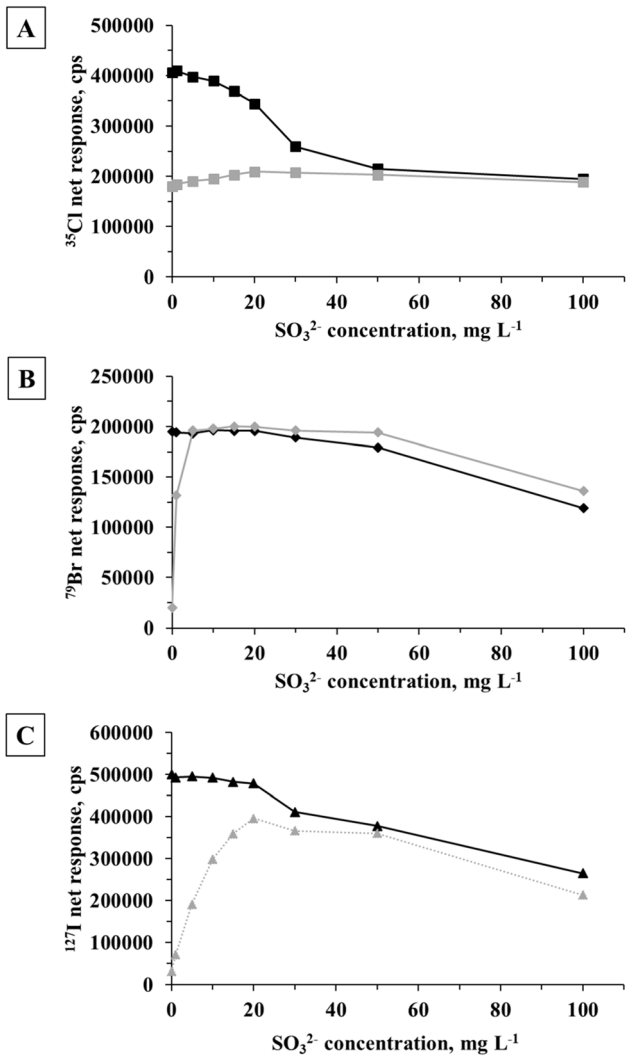

Fig. 7 Influence of the SO_3^{2-} concentration on PVG response from: (A) 5 mg L^{-1} Cl^- (■) or ClO_3^- (■); (B) 10 μg L^{-1} Br^- (◆) or BrO_3^- (◆); and (C) 2 μg L^{-1} I^- (▲) or IO_3^- (▲) in a medium of 1% v/v acetic acid/20 mg L^{-1} Cu^{2+}. Error bars presenting the standard deviation ($n = 3$) are typically buried within the signal marker.

Generation efficiency is significantly enhanced for BrO_3^- in the range 5 to 50 mg L^{-1} of added SO_3^{2-}, providing a response similar to that obtained with Br^- (Fig. 7B). Furthermore, the addition of SO_3^{2-} did not interfere with generation of Br^- up to a concentration of 50 mg L^{-1}. In the presence of 100 mg L^{-1} SO_3^{2-}, 40% and 30% signal suppressions occurred for Br^- and BrO_3^-, respectively.

Maximum response from IO_3^- was obtained using 20 mg L^{-1} of SO_3^{2-} (differing by 20% compared to the signal obtained from I^-, Fig. 7C). At concentrations exceeding 40 mg L^{-1} SO_3^{2-}, a decline in signal intensity was observed for both I species.

Although enhanced PVG generation efficiencies achieved for BrO_3^- and IO_3^- in an acetic acid/Cu^{2+}/SO_3^{2-} medium render the PVG-ICP-MS methodology a feasible approach for the determination of total Br and I in samples wherein both their halide and halate species may be present, this approach remains entirely unsatisfactory for total Cl. Noteworthy from Fig. 7 is that at a SO_3^{2-} concentration of 50 mg L^{-1} it would appear that each of the tested halates is converted to the corresponding halide to provide the same response for both species, albeit at an overall suppressed response in each case.

3.4 Figures of merit

Figures of merit for the halides, summarized in Table 2, were evaluated under optimized compromise conditions employing a solution of 1% v/v acetic acid containing 20 mg L^{-1} Cu^{2+} as the PVG medium. Comparative performance metrics with conventional sample PN are also presented. Calibration curves for both PVG and PN sample introduction were constructed in the ranges 0.1 to 7.5 mg L^{-1} for Cl^-, 0.1 to 20 μg L^{-1} for Br^- and 0.01 to 5 μg L^{-1} for I^-, resulting in coefficients of determination (R^2) higher than 0.999 for all elements using either sample introduction system. The PVG method demonstrated an approximate 3-, 40- and 30-fold increase in sensitivity for Cl^-, Br^- and I^-, respectively, compared to PN. This resulted in similar enhancements in their limits of detection (LODs). Although the net sensitivity for Br^- at *m*/*z* 81 was indistinguishable from that observed at *m*/*z* 79, the elevated background from the rising edge of $^{81}Ar_2H^+$ and from the tail of $^{80}Ar^{2+}$ resulted in 4-fold degradation in the LOD for ^{81}Br and elevated signal intensities evident for both PN and PVG blanks.

The relatively high blank levels for the halides present in the acetic acid used in this study compromises the achievable LODs when employing PVG methodology. Method blanks (arising from PVG matrix constituents) corresponded to concentrations of 0.18 mg L^{-1} for ^{35}Cl, 0.24 μg L^{-1} for ^{79}Br and 0.03 μg L^{-1} for ^{127}I. In an effort to reduce their magnitude, TAMA AA-100 ultrapure acetic acid was tested. Although a reduction of approximately 40% in the blank value for I^- was achieved, a significant contamination for Br^-, estimated at 30 μg L^{-1}, persisted. Furthermore, no difference in blanks were evident for Cl^- compared to the ACS-grade acetic acid. Thus, given the demands for achieving simultaneous determination of the halides using this method, the ACS-grade acetic acid was retained for application to subsequent analyses.

Overall efficiencies (generation and transport) were estimated following an analysis of the residual Cl, Br and I content

Table 2 Figures of merit for Cl^-, Br^- and I^- obtained using aerosol-assisted PVG-ICP-MS from a generation medium of 1% v/v acetic acid containing 20 mg L^{-1} Cu^{2+}

	^{35}Cl		^{79}Br		^{81}Br		^{127}I	
Parameter	PVG	PN	PVG	PN	PVG	PN	PVG	PN
Sensitivity[a] ($\times 10^{-5}$)	1.2	0.37	0.25	0.007	0.25	0.007	3.5	0.11
Blank, cps	21 500	16 500	6000	4000	31 500	32 400	8800	4900
LOD[b], pg mL^{-1}	4200	9500	6.3	270	27	1300	1.9	30
Precision[c], %	5	4	2	3	3	2	3	3
PVG efficiency[d], %	10 ± 3	—	99 ± 2	—	99 ± 2	—	90 ± 3	—

[a] Slope of the calibration function, expressed as cps ppm^{-1} for Cl and cps ppb^{-1} for Br and I. [b] LOD = $3s/m$, where m is the slope of the calibration function and s is the standard deviation of ten replicate measurements of the 1% v/v ACS-grade acetic acid + 20 mg L^{-1} Cu^{2+} blank. [c] Relative standard deviation of measurement of 10 consecutive samples containing 5 mg L^{-1} for Cl^-, 10 μg L^{-1} for Br^- and 1 μg L^{-1} for I^- in 1% v/v ACS-grade acetic acid + 20 mg L^{-1} Cu^{2+}. [d] PVG efficiency, estimated from an analysis of the residual Cl, Br and I in the waste solution carefully collected from the UV-assisted spray chamber following sample irradiation.

in the waste solution carefully collected from the UV-assisted spray chamber. Once a steady-state signal for a solution containing 5 mg L^{-1} Cl^-, 10 μg L^{-1} Br^-, and 2 μg L^{-1} I^- in 1% v/v acetic acid and 20 mg L^{-1} Cu^{2+} had been achieved, the generated waste was collected and re-analyzed by PVG-ICP-MS.

Sample introduction efficiency achieved with PN was estimated to be between 2–3% using a mass balance difference between that of solution uptake and waste recovery. For PVG, the 10 ± 3% efficiency estimated for Cl^- is improved relative to PN but notably lower than the earlier reported value of 80% obtained using a flow-through lamp as the photoreactor,[2] highlighting the importance of the sample irradiation time on PVG synthesis of CH_3Cl (approximately 3 s within the UV-assisted spray chamber *vs.* 45 s within the flow-through lamp). Despite this, the LOD achieved for Cl^- can be considered fit-for-purpose (4.2 μg L^{-1}), providing a wide range of applicability due to the often-elevated chlorine concentrations typically found in many different types of real samples.

Efficiencies of 99 ± 2 and 90 ± 3% estimated for Br^- and I^-, respectively, represent a significant improvement over standard PN introduction and are consistent with those reported in previous studies, in which both the flow-through lamp and the UV-assisted spray chamber were employed.[29,32] These results indicate that the short sample irradiation time with the UV-assisted spray chamber does not impair the generation efficiency of these two elements.

PVG efficiencies for the generation of Cl, Br and I from their respective halates were no better than 5% in the absence of added SO_3^-. As discussed earlier, addition of 20 mg L^{-1} of SO_3^- to the generation medium enhanced efficiency for BrO_3^- and IO_3^- without affecting response from Br^- and I^-. As a result, 40- and 26-fold increases in sensitivity compared to conventional PN sample introduction were obtained for Br and I detection following their generation from BrO_3^- and IO_3^- using 1% v/v acetic acid containing 20 mg L^{-1} Cu^{2+} and 20 mg L^{-1} SO_3^{2-}. This resulted in an overall PVG efficiency of 99 ± 1% for BrO_3^- and 86 ± 2% for IO_3^-. As noted earlier, use of SO_3^{2-} did not prove efficacious for ClO_3^-.

Precision of measurement was reflected in the relative standard deviation of the mean signals derived from 10 consecutive samples containing 5 mg L^{-1} Cl^-, 10 μg L^{-1} Br^- and 1 μg L^{-1} I^-. Results are in the range of 2 to 5% for both the PVG and PN analyte introduction approaches.

A short justification of the relatively high flow rate for PVG sample introduction used in this study is warranted at this point. Although plasma-based analyses are often developed with low flow applications in mind, which are beneficial to sample consumption and alleviation of issues relating to matrix deposition on interface components, the highest sample flow rate consistent with generation of a stable aerosol is desirable for PVG work. Aerosols permitting efficient photolysis reactions on a short time scale and rapid separation of synthesized analyte from the liquid phase to enhance product transport to the plasma are desirable since signal response is proportional to flow rate (all other conditions being satisfied), yielding optimal analytical metrics.

3.5 Simultaneous determination of total Cl, Br and I in real samples by aerosol-assisted PVG-ICP-MS

Application of PVG-ICP-MS for the analysis of real samples often remains a significant challenge due to severe interferences induced by common reagents used for their preparation, particularly HNO_3. For the determination of the halogens, the use of MIC has been widely explored due to a number of attractive factors, including the elimination of the risk of their loss as volatile HCl, HBr and HI, rapid sample throughput, capacity to digest relatively high sample masses, enhanced digestion efficiencies (yielding digests with low residual carbon content), and the low blank levels achieved through the use of dilute reagents or even water as the absorbing medium.[1,24] These characteristics render MIC particularly appealing as a sample preparation method for subsequent halogen determinations by PVG-ICP-MS. The methodology developed herein was thus evaluated by analysis of four different CRM matrices digested using MIC: NIST SRM 1515 (Apple Leaves), NIST SRM 1549 (Non-fat Milk Powder), NIST SRM 1632c (Coal), and NRCC CRM DORM-5 (Fish Protein).

The use of alkaline reagents as absorber solutions is recommended for the quantitative recovery and stabilization of halogens following MIC, and dilute solutions of NH_4OH are

Table 3 Results[a] for total Cl, Br and I in CRMs by aerosol-assisted PVG-ICP-MS

	Cl		Br		I	
Sample[a], μg g^{-1}	Determined	Certified value	Determined	Certified value	Determined	Certified value
NIST SRM 1515	564 ± 12	582 ± 15	1.77 ± 0.12	1.8[b]	0.318 ± 0.010	0.3[b]
NIST SRM 1549	1.02 ± 0.03[c]	1.09 ± 0.02[c]	12.1 ± 0.9	12[b]	2.84 ± 0.08	3.38 ± 0.02
NIST SRM 1632c	0.117 ± 0.002[c]	0.1139 ± 0.0041[c]	16.2 ± 0.3	18.7 ± 0.4[d]	—	—
NRCC DORM-5	14 100 ± 700	12 220[b]	52.6 ± 4.4	50.7[b]	7.13 ± 1.63	7.5 ± 1.4[d]

[a] Values expressed for dry weight basis as mean ± standard deviation, $n = 3$. [b] Information value. [c] Values expressed in % w/w. [d] Reference value.

typically used for this purpose.[24] However, as discussed in Section 3.3, NH_4OH induces signal suppressions for PVG of Cl^-, Br^- and I^- when present at concentrations above 5, 25, and 100 mmol L^{-1}, respectively. In this work, a 50 mmol L^{-1} NH_4OH solution was used to absorb the analytes, giving rise to a final concentration of 12 mmol L^{-1} NH_4OH in the prepared digests. As a consequence of poor PVG of the analytes at such a NH_4OH concentration, a minimum final dilution factor of at least 4-fold is required to ensure an interference-free response. Considering the impact of nitrate on PVG, and the typical use of 6 mol L^{-1} NH_4NO_3 as the combustion aid for MIC, a final digest containing 12 mmol L^{-1} NO_3^- would be expected. This contributes to significant interferences (Section 3.3). In an effort to minimize the final NO_3^- concentration, the NH_4NO_3 igniter was reduced to 3 mol L^{-1} (providing a concentration of 6 mmol L^{-1} in the final sample digests). Despite the expected longer sample ignition time required using 3 mol L^{-1} NH_4NO_3 (*vs.* 6 mol L^{-1}),[50] effective combustion appeared evident for all samples without significant undigested material or sample residues. In this way, a maximum 4-fold dilution factor is sufficient to mitigate interferences induced by both NH_4OH and NO_3^-. Furthermore, dilution should not compromise the quantification of the elements in the tested samples, given their expected analyte concentrations and method LODs.

Analytical results are summarized in Table 3. Calibration was accomplished against external matrix free multielement halide standards prepared in the same PVG medium. With the notable exception of iodine in NIST SRM 1549 (Milk powder), there is generally good agreement between determined and certified values (*t* test, confidence level of 95%) or information/reference values for the halogens in these materials, supporting the accuracy of the proposed method. Results for I in NIST SRM 1549 are biased significantly low compared to the certified value. Subsequent studies were performed by adding 20 mg L^{-1} SO_3^- as a second mediator (data not presented in Table 3), but similar results were obtained, indicating that the lower concentration is not related to the presence of IO_3^- endogenous to the sample or arising from the MIC process. This finding was consistent with the results of a previous study[44] reporting that halate species are not formed during the MIC process. This conclusion was further corroborated by subsequent analysis of NRCC GSEA-1 (Ground Seaweed) CRM in the laboratory of the authors at UFSM. Statistical agreement of results generated by ion chromatography coupled to PN ICP-MS indicated the presence of only halide species, permitting its accurate quantitation against external halide-based standards.

Attention then focused on the earlier decision to minimize the final concentration of NO_3^- in the sample digests by utilizing 3.0 mol L^{-1} NH_4NO_3 as the ignitor for MIC instead of the recommended 6.0 mol L^{-1}. For NIST SRM 1549, values of 2.73 ± 0.14 and 3.21 ± 0.17 μg g^{-1} were generated for I by calibration with PN ICP-MS on samples prepared in 3 and 6 mol L^{-1} NH_4NO_3, respectively, completely accounting for the discrepancy with the certified value of 3.38 ± 0.02 μg g^{-1}.

4 Conclusion

A rapid, accurate, precise and simple method for the simultaneous determination of Cl, Br and I in real samples was developed based on use of a UV-assisted spray chamber as photoreactor for PVG sample introduction and ICP-MS detection. Using Cu^{2+} as mediator (in 1% v/v acetic acid medium), LODs were enhanced 3-, 40- and 30-fold compared to conventional PN for Cl^-, Br^- and I^-, respectively. Most noteworthy is that PVG efficiency for only Cl^- is severely limited by the short sample irradiation time within the photoreactor as compared to that with use of a flow through lamp. The generally high efficiency may be supportive of recent findings regarding the unique environments produced within microdroplets by sample aerosolization, in which reaction rates may be accelerated due to altered physical properties relative to the bulk medium.[40–42,51] A full understanding of the impact of such an environment on PVG reactions is currently unknown. In this context, it may be instructive to undertake further studies to elucidate the influence of the microdroplet environment on these photochemical reactions by, for example, using means to alter the droplet diameter distributions.

Although interferences from NO_3^- are inherent to many PVG reactions and have impact even at low concentrations, they could be minimized using the UV-assisted spray chamber. A low solution pH may be beneficial in reducing the impact of NO_3^- with this system. Also noteworthy was that the alkaline pH obtained at concentrations of NH_4OH higher than 5 mmol L^{-1} significantly influenced PVG from halides, with a pronounced decrease in response from Cl^-, possibly attributed to availability of free Cu^{2+} (due to formation of $Cu(OH)_2$ or $[Cu(NH_3)_4]^{2+}$). This affected PVG of Br^- to a lesser extent whereas PVG of I^- was suppressed only at higher concentrations of NH_4OH (>100 mmol L^{-1}).

Photochemical generation of ClO_3^-, BrO_3^- and IO_3^- introduced unresolved issues with the use of the UV-assisted spray chamber that could only be partly improved by addition of SO_3^{2-} as a secondary modifier. Response from BrO_3^- and IO_3^- ultimately achieved 40- and 26-fold enhancements in sensitivity, respectively, compared to PN. This approach should prove useful when both Br^- and BrO_3^- or I^- and IO_3^- are present in the sample, enabling the use of the aerosol-assisted PVG-ICP-MS as a detection technique when coupled with ion chromatographic separation for rigorous speciation analysis. However, it is important to consider potential interferences caused by SO_3^{2-} on their PVG generation. Further investigations are required to improve the photochemical reduction of ClO_3^- in the presence of SO_3^{2-}, such as by use of a flow-through photoreactor.

Despite the above identified difficulties, the determination of total halogen content in samples subjected to sample preparation by MIC yields results with fit-for-purpose accuracy for a wide variety of sample matrices based on use of a simple PVG medium. Fig. 7 suggests that in samples where halite species are suspected, this methodology should still be capable of accurate analyses of total halogen content in the presence of SO_3^{2-} at an added concentration of 50 mg L^{-1} if a loss of 50% in generation efficiency can be tolerated.

Data availability

Data supporting the experimental findings of this study are presented within the article and ESI;† those mentioned by way of a simple summary statement are available from the corresponding author upon reasonable request.

Conflicts of interest

There are no conflicts to declare.

Acknowledgements

The authors are grateful to Coordenação de Aperfeiçoamento de Pessoal de Nível Superior (CAPES, Finance Code 001) for the sandwich PhD fellowship process number 8887.898440/2023-00 (CAPES PrInt) awarded to Gustavo Rossato Bitencourt. This study was financed in part by the Conselho Nacional de Desenvolvimento Científico e Tecnológico (CNPq, grant 314254/2023-4, by P. A. Mello).

References

1 E. M. M. Flores, P. A. Mello, S. R. Krzyzaniak, V. H. Cauduro and R. S. Picoloto, Challenges and trends for halogen determination by inductively coupled plasma mass spectrometry: A review, *Rapid Commun. Mass Spectrom.*, 2020, **34**, e8727.

2 J. Hu, R. E. Sturgeon, K. Nadeau, X. Hou, C. Zheng and L. Yang, Copper Ion Assisted Photochemical Vapor Generation of Chlorine for Its Sensitive Determination by Sector Field Inductively Coupled Plasma Mass Spectrometry, *Anal. Chem.*, 2018, **90**, 4112–4118.

3 ASTM D5127-13, *Standard Guide for Ultra-Pure Water Used in the Electronics and Semiconductor Industries*, ASTM International, West Conshohocken, PA, 2013.

4 A. S. McCall, C. F. Cummings, G. Bhave, R. Vanacore, A. Page-McCaw and B. G. Hudson, Bromine Is an Essential Trace Element for Assembly of Collagen IV Scaffolds in Tissue Development and Architecture, *Cell*, 2014, **157**, 1380–1392.

5 R. C. Woody, Bromide Therapy for Pediatric Seizure Disorder Intractable to Other Antiepileptic Drugs, *J. Child Neurol.*, 1990, **5**, 65–67.

6 S. Pavelka, Metabolism of Bromide and Its Interference with the Metabolism of Iodine, *Physiol. Res.*, 2004, **53**, 81–90.

7 L. Patrick, Iodine: Deficiency and therapeutic considerations, *Alternative Med. Rev.*, 2008, **13**, 116–127.

8 L. S. F. Pereira, M. F. Pedrotti, P. D. Vecchia, J. S. F. Pereira and E. M. M. Flores, A simple and automated sample preparation system for subsequent halogens determination: Combustion followed by pyrohydrolysis, *Anal. Chim. Acta*, 2018, **1010**, 29–36.

9 S. R. Krzyzaniak, R. F. Santos, F. M. Dalla Nora, S. M. Cruz, E. M. M. Flores and P. A. Mello, Determination of halogens and sulfur in high-purity polyimide by IC after digestion by MIC, *Talanta*, 2016, **158**, 193–197.

10 A. L. H. Müller, C. C. Müller, F. G. Antes, J. S. Barin, V. L. Dressler, E. M. M. Flores and E. I. Müller, Determination of Bromide, Chloride, and Fluoride in Cigarette Tobacco by Ion Chromatography after Microwave-Induced Combustion, *Anal. Lett.*, 2012, **45**, 1004–1015.

11 A. D'Ulivo, E. Pagliano, M. Onor, E. Pitzalis and R. Zamboni, Vapor Generation of Inorganic Anionic Species After Aqueous phase Alkylation with Trialkyloxonium Tetrafluoroborates, *Anal. Chem.*, 2009, **81**, 6399–6406.

12 E. Pagliano, J. Meija, J. Ding, R. E. Sturgeon, A. D'Ulivo and Z. Mester, Novel Ethyl-Derivatization Approach for the Determination of Fluoride by Headspace Gas Chromatography/Mass Spectrometry, *Anal. Chem.*, 2013, **85**, 877–881.

13 Z. Gajdosechova, Z. Mester and E. Pagliano, A rapid and sensitive method for the determination of inorganic chloride in oil samples, *Anal. Chim. Acta*, 2019, **1064**, 40–46.

14 D. Desideri, M. A. Meli and C. Roselli, Determination of essential and non-essential elements in some medicinal plants by polarised X ray fluorescence spectrometer (EDPXRF), *Microchem. J.*, 2010, **95**, 174–180.

15 S. Yamasaki, A. Takeda, T. Watanabe, K. Tagami, S. Uchida, H. Takata, Y. Maejima, N. Kihou and N. Tsuchiya, Bromine and iodine in Japanese soils determined with polarizing energy dispersive X-ray fluorescence spectrometry, *Soil Sci. Plant Nutr.*, 2015, **61**, 751–760.

16 U. Heitmann, H. Becker-Ross, S. Florek, M. D. Huang and M. Okruss, Determination of non-metals *via* molecular absorption using high-resolution continuum source absorption spectrometry and graphite furnace atomization, *J. Anal. At. Spectrom.*, 2006, **21**, 1314–1320.

17 F. Cacho, L. Machynak, M. Nemecek and E. Beinrohr, Determination of bromide in aqueous solutions *via* the TlBr molecule using high-resolution continuum source graphite furnace molecular absorption spectrometry, *Spectrochim. Acta, Part B*, 2018, **144**, 63–67.
18 M. Schneider, B. Welz, M.-D. Huang, H. Becker-Ross, M. Okruss and E. Carasek, Iodine determination by high-resolution continuum source molecular absorption spectrometry – A comparison between potential molecules, *Spectrochim. Acta, Part B*, 2019, **153**, 42–49.
19 T. Taflik, F. A. Duarte, É. L. M. Flores, F. G. Antes, J. N. G. Paniz, É. M. M. Flores and V. L. Dressler, Determination of bromine, fluorine and iodine in mineral supplements using pyrohydrolysis for sample preparation, *J. Braz. Chem. Soc.*, 2012, **23**, 488–495.
20 T. S. Nunes, C. C. Muller, P. Balestrin, A. L. H. Muller, M. F. Mesko, P. de A. Mello and E. I. Muller, Determination of chlorine and sulfur in high purity flexible graphite using ion chromatography (IC) and inductively coupled plasma optical emission spectrometry (ICP OES) after pyrohydrolysis sample preparation, *Anal. Methods*, 2015, **7**, 2129–2134.
21 F. G. Antes, J. S. F. Pereira, M. S. P. Enders, C. M. M. Moreira, E. I. Müller, E. M. M. Flores and V. L. Dressler, Pyrohydrolysis of carbon nanotubes for Br and I determination by ICP-MS, *Microchem. J.*, 2012, **101**, 54–58.
22 J. T. P. Barbosa, C. M. M. Santos, L. dos Santos Bispo, F. H. Lyra, J. M. David, M. das G. A. Korn and E. M. M. Flores, Bromine, Chlorine, and Iodine Determination in Soybean and its Products by ICP-MS After Digestion Using Microwave-Induced Combustion, *Food Anal. Methods*, 2013, **6**, 1065–1070.
23 E. Tjabadi and N. Mketo, Recent developments for spectrometric, chromatographic and electroanalytical determination of the total sulphur and halogens in various matrices, *TrAC, Trends Anal. Chem.*, 2019, **118**, 207–222.
24 M. F. Mesko, V. C. Costa, R. S. Picoloto, C. A. Bizzi and P. A. Mello, Halogen determination in food and biological materials using plasma-based techniques: challenges and trends of sample preparation, *J. Anal. At. Spectrom.*, 2016, **31**, 1243–1261.
25 R. E. Sturgeon, Photochemical vapor generation: A radical approach to analyte introduction for atomic spectrometry, *J. Anal. At. Spectrom.*, 2017, **32**, 2319–2340.
26 R. E. Sturgeon, in *Vapor Generation Techniques for Trace Elements Analysis*, ed. A. D'Ulivo and R. E. Sturgeon, Elsevier, Amsterdam, 2022, pp. 213–263.
27 R. E. Sturgeon and P. Grinberg, Some speculations on the mechanisms of photochemical vapor generation, *J. Anal. At. Spectrom.*, 2012, **27**, 222–231.
28 P. Grinberg and R. E. Sturgeon, Ultra-trace determination of iodine in sediments and biological material using UV photochemical generation-inductively coupled plasma mass spectrometry, *Spectrochim. Acta, Part B*, 2009, **64**, 235–241.
29 P. Grinberg and R. E. Sturgeon, Photochemical vapor generation of iodine for detection by ICP-MS, *J. Anal. At. Spectrom.*, 2009, **24**, 508–514.
30 R. M. Oliveira, B. S. Soares and D. L. G. Borges, A simple dilute-and-shoot approach using UV photochemical vapor generation for the determination of iodine in alcoholic beverages by ICP-MS, *J. Food Compos. Anal.*, 2021, **95**, 103655.
31 R. E. Sturgeon, Detection of bromine by ICP- oa -ToF-MS following photochemical vapor generation, *Anal. Chem.*, 2015, **87**, 3072–3079.
32 R. M. De Oliveira, D. L. G. Borges, P. Grinberg, Z. Mester and R. E. Sturgeon, Copper-ion assisted photochemical vapor generation of bromide and bromate, *J. Anal. At. Spectrom.*, 2021, **36**, 1235–1243.
33 R. E. Sturgeon and E. Pagliano, Evidence for photochemical synthesis of fluoromethane, *J. Anal. At. Spectrom.*, 2020, **35**, 1720–1726.
34 A. Bakač, Effects of halide ions and carbon monoxide on the reactions of iron(III) with alkyl radicals, *Croat. Chem. Acta*, 2001, **74**, 633–640.
35 J. M. Carraher, O. Pestovsky and A. Bakac, Transition metal ion-assisted photochemical generation of alkyl halides and hydrocarbons from carboxylic acids, *Dalton Trans.*, 2012, **41**, 5974–5980.
36 D. Leonori and R. E. Sturgeon, A unified approach to mechanistic aspects of photochemical vapor generation, *J. Anal. At. Spectrom.*, 2019, **34**, 636–654.
37 J. Hu, H. Chen, X. Jiang and X. Hou, Photochemical Vapor Generation of Halides in Organic-Acid-Free Media: Mechanism Study and Analysis of Water Samples, *Anal. Chem.*, 2021, **93**, 11151–11158.
38 R. E. Sturgeon, S. N. Willie and Z. Mester, UV/spray chamber for generation of volatile photo-induced products having enhanced sample introduction efficiency, *J. Anal. At. Spectrom.*, 2006, **21**, 263–265.
39 H. Matusiewicz, M. Ślachciński, P. Pawłowski and M. Portalski, Evaluation of Five Phase Digitally Controlled Rotating Field Plasma Source for Photochemical Mercury Vapor Generation Optical Emission Spectrometry, *Anal. Sci.*, 2015, **31**, 987–995.
40 J. K. Lee, D. Samanta, H. G. Nam and R. N. Zare, Micrometer-Sized Water Droplets Induce Spontaneous Reduction, *J. Am. Chem. Soc.*, 2019, **141**, 10585–10589.
41 H. Xiong, J. K. Lee, R. N. Zare and W. Min, Strong Electric Field Observed at the Interface of Aqueous Microdroplets, *J. Phys. Chem. Lett.*, 2020, **11**, 7423–7428.
42 M. Girod, E. Moyano, D. I. Campbell and R. G. Cooks, Accelerated bimolecular reactions in microdroplets studied by desorption electrospray ionization mass spectrometry, *Chem. Sci.*, 2011, **2**, 501–510.
43 R. S. Picoloto, M. Doneda, E. L. M. Flores, M. F. Mesko, E. M. M. Flores and P. A. Mello, Simultaneous determination of bromine and iodine in milk powder for adult and infant nutrition by plasma based techniques after digestion using microwave-induced combustion, *Spectrochim. Acta, Part B*, 2015, **107**, 86–92.

44 É. M. M. Flores, M. F. Mesko, D. P. Moraes, J. S. F. Pereira, P. A. Mello, J. S. Barin and G. Knapp, Determination of Halogens in Coal after Digestion Using the Microwave-Induced Combustion Technique, *Anal. Chem.*, 2008, **80**, 1865–1870.

45 H. Coutinho de Jesus, P. Grinberg and R. E. Sturgeon, System optimization for determination of cobalt in biological samples by ICP-OES using photochemical vapor generation, *J. Anal. At. Spectrom.*, 2016, **31**, 1590–1604.

46 G. S. Lopes, R. E. Sturgeon, P. Grinberg and E. Pagliano, Evaluation of approaches to the abatement of nitrate interference with photochemical vapor generation, *J. Anal. At. Spectrom.*, 2017, **32**, 2378–2390.

47 L. Velásquez-Yévenes and R. Ram, The aqueous chemistry of the copper-ammonia system and its implications for the sustainable recovery of copper, *Clean. Eng. Technol.*, 2022, **9**, 100515.

48 L. Yang, L. He, J. Xue, Y. Ma, Y. Shi, L. Wu and Z. Zhang, UV/SO32− based advanced reduction processes of aqueous contaminants: Current status and prospects, *Chem. Eng. J.*, 2020, **397**, 125412.

49 B. D. Fennell, S. P. Mezyk and G. McKay, Critical Review of UV-Advanced Reduction Processes for the Treatment of Chemical Contaminants in Water, *ACS Environ. Au*, 2022, **2**, 178–205.

50 M. F. Pedrotti, L. S. F. Pereira, C. A. Bizzi, J. N. G. Paniz, J. S. Barin and E. M. M. Flores, Microwave-induced combustion: Thermal and morphological aspects for understanding the mechanism of ignition process for analytical applications, *Talanta*, 2017, **174**, 64–71.

51 Q. He, N. Zhang, Y. Qiao, C. Li and J. Zhang, Vapor generation of mercury and methylmercury in aqueous microdroplets produced by pneumatic nebulization, *J. Anal. At. Spectrom.*, 2022, **37**, 1894–1901.